Revista ALCONPAT
www.revistaalconpat.org
eISSN 2007-6835
Revista de la Asociación Latinoamericana de Control de Calidad, Patología y Recuperación de la Construcción

Structural assessment of an existing reinforced concrete building using a complementary approach based on visual inspection, non-destructive testing, and load testing.

J. G. Peredo Villarroel[1], C. D. Rojas Quispe[1], J. Lafuente Fernandez[1], J. Ticona Martinez[1], H. N. Callao Corrales[1], R. Solis[1], J. H. Aquino Rocha[1]*
*Contact author: j.aquino@umss.edu.bo
DOI: https://doi.org/10.21041/ra.v16i2.1013

Received: 19/01/2026 | Received in revised form: 08/04/2026 | Accepted: 11/04/2026 | Published: 01/05/2026

ABSTRACT

This study aims to evaluate the structural suitability of an existing reinforced concrete building. The methodology is based on the integration of visual inspection, non-destructive testing (rebound hammer, ultrasonic pulse velocity, and infrared thermography), and load testing on slabs. The results reveal unfavorable conditions, with material heterogeneity, internal degradation, and non-uniform structural behavior. Limitations include the absence of destructive testing and detailed structural information. The main contribution of the study lies in the integration of assessment techniques at different levels of the structural system. The structure cannot be considered fully suitable for use in its current condition.

Keywords: Visual inspection; Rebound hammer; UPV; Infrared thermography; Load testing.

Cite as: Peredo Villarroel, J. G., Rojas Quispe, C. D., Lafuente Fernandez, J., Ticona Martinez, J., Callao Corrales, H. N., Solis, R., Aquino Rocha, J. H. (2026), "*Structural assessment of an existing reinforced concrete building using a complementary approach based on visual inspection, non-destructive testing, and load testing.*" Revista ALCONPAT, 16 (2). pp. 268 – 291, DOI: https://doi.org/10.21041/ra.v16i2.1013

[1] Departamento de Ingeniería Civil, Facultad de Ciencias y Tecnología, Universidad Mayor de San Simón, Cochabamba, Bolivia.

Contribution of each author
In this work, all authors (J.G. Peredo Villarroel, C.D. Rojas Quispe, J. Lafuente Fernández, J. Ticona Martínez, H.N. Callao Corrales, R. Solis, and J.H.A. Rocha) contributed equally to the different stages of the study, including conceptualization, experimental execution, data collection and analysis, as well as manuscript writing and revision, with an estimated contribution of 14.3% per author.

Discussions and subsequent corrections to the publication
Any dispute, including the replies of the authors, will be published in the first issue of 2027 provided that the information is received before the closing of the third issue of 2026.

Evaluación estructural de una edificación existente de hormigón armado mediante un enfoque complementario de inspección visual, ensayos no destructivos y prueba de carga

RESUMEN

El presente estudio tiene como objetivo evaluar la aptitud estructural de una edificación existente de hormigón armado. La metodología se basa en la integración de inspección visual, ensayos no destructivos (esclerometría, velocidad de pulso ultrasónico y termografía infrarroja) y prueba de carga en losas. Los resultados evidencian un estado de conservación desfavorable, con heterogeneidad del material, degradación interna y un comportamiento estructural no uniforme. Como limitaciones, se reconoce la ausencia de ensayos destructivos y de información estructural detallada. La originalidad del estudio radica en la integración de técnicas de evaluación aplicadas a diferentes niveles del sistema estructural. Se concluye que la estructura no es plenamente apta para su uso en su estado actual.

Palabras clave: inspección visual; esclerómetro; VPU; termografía infrarroja; prueba de carga.

Avaliação estrutural de uma edificação existente de concreto armado por meio de uma abordagem complementar de inspeção visual, ensaios não destrutivos e prova de carga

RESUMO

Este estudo tem como objetivo avaliar a aptidão estrutural de uma edificação existente de concreto armado. A metodologia baseia-se na integração de inspeção visual, ensaios não destrutivos (esclerometria, velocidade de pulso ultrassônico e termografia infravermelha) e prova de carga em lajes. Os resultados evidenciam um estado de conservação desfavorável, com heterogeneidade do material, degradação interna e comportamento estrutural não uniforme. Como limitações, destaca-se a ausência de ensaios destrutivos e de informações estruturais detalhadas. A originalidade reside na integração de técnicas de avaliação em diferentes níveis do sistema estrutural. Conclui-se que a estrutura não é plenamente apta para uso em sua condição atual.

Palavras-chave: inspeção visual; esclerometria; VPU; termografia infravermelha; prova de carga.

1. INTRODUCTION

The assessment of the structural condition of existing reinforced concrete buildings remains a major challenge in civil engineering, particularly for structures exposed to prolonged aggressive environmental conditions and for those in which the original structural design information is incomplete or unavailable. This situation increases the uncertainty associated with determining the mechanical properties of the material and the structural behavior, thereby complicating decision-making regarding safety and in-service performance (Bungey & Grantham, 2006; Bortolini & Forcada, 2018). In this context, it is necessary to ensure an appropriate structural assessment without resorting to destructive interventions, which requires moving beyond traditional evaluation approaches as well as adopting comprehensive and updated methodologies capable of generating reliable and consistent information for existing and deteriorated structures (De Domenico *et al*., 2022; Diaferio & Varona, 2024; Watt, 2025).

In professional practice, the structural evaluation of existing buildings relies on the interpretation of results obtained through indirect testing methods, particularly non-destructive testing (NDT), complemented by the judgment of the responsible inspector or evaluator (Ghosn *et al*., 2016). The most commonly used NDT methods include visual inspection, ground-penetrating radar (GPR), rebound hammer testing, ultrasonic pulse velocity (UPV), infrared thermography, and electrical resistivity of concrete. These methods are characterized by being non-invasive, rapidly applicable, and capable of providing a preliminary assessment of the condition of both concrete and reinforcement. They offer information on material quality, the presence of internal heterogeneities or discontinuities, as well as durability conditions and the potential risk of reinforcement corrosion (Ali-Benyahia *et al*., 2023; Krentowski *et al*., 2023; Boccacci *et al*., 2024). Collectively, these techniques enable the identification of deteriorated zones, variations in compactness, and the presence of moisture, thereby providing relevant information for structural diagnosis and technical decision-making (Gupta *et al*., 2022; Alqurashi *et al*., 2022).

However, despite their widespread use, NDT methods present several limitations, as they are indirect techniques sensitive to factors such as carbonation, moisture content, surface condition of the concrete, and its heterogeneity. These influences may lead to overestimation or underestimation of mechanical properties, particularly in older structures with advanced deterioration, thereby compromising the reliability of NDT as a standalone tool for supporting decisions related to structural repair and/or strengthening (Malhotra & Carino, 2003; Abdollahi-Mamoudan *et al*., 2025).

On the other hand, load testing constitutes a direct experimental tool for evaluating the behavior of existing structures, as it allows verification of the global response of the building under controlled service conditions through the measurement of deflections, residual deformations, and elastic recovery (American Concrete Institute, 2025). Among the various standards that can be applied for load testing, ACI 318 (American Concrete Institute, 2025) provides an objective framework to assess whether the observed behavior is consistent with safe structural performance. However, load testing is typically applied as an independent procedure, without integration with results obtained from other testing methods, such as NDT.

The scientific and technical literature shows a limited availability of complementary methodological approaches that allow a direct correlation between results obtained from NDT and the structural behavior observed during load testing (Olaszek *et al*., 2014; Abedin *et al*., 2022). This limitation reduces the practical applicability of NDT in the evaluation of existing structures, particularly in those exhibiting advanced deterioration associated with carbonation processes and loss of durability, where uncertainty regarding actual structural performance is high.

In this context, the present study aims to evaluate the structural suitability of an existing reinforced concrete building through an approach based on the integration of visual inspection, NDT, and load testing, in order to support technical decision-making regarding its potential use, intervention, or rehabilitation. The approach is developed through a case study of a building with advanced deterioration, in which the results obtained from the different techniques are analyzed jointly, allowing for a more representative structural diagnosis of the actual condition of the building. The main contribution of this study lies in demonstrating that the integration of results from NDT and load testing enables the identification of the scope and limitations of each technique, thereby strengthening the structural assessment process and supporting decision-making in contexts with limited information.

2. METHODOLOGY

This work is presented as an applied case study with a methodological focus, whose objective is to evaluate the structural suitability of an existing building through the integration of different assessment techniques. The study has a diagnostic nature, as it analyzes the structural condition of a specific building, and at the same time a demonstrative purpose, as it evidences the applicability of the proposed methodology under real field conditions.

2.1 Proposed methodological approach

The adopted methodology is based on the complementary application of NDT and static load testing, constituting a proposal for the structural assessment of an existing structure through a case study approach. Figure 1 presents the detailed procedure followed in this study.

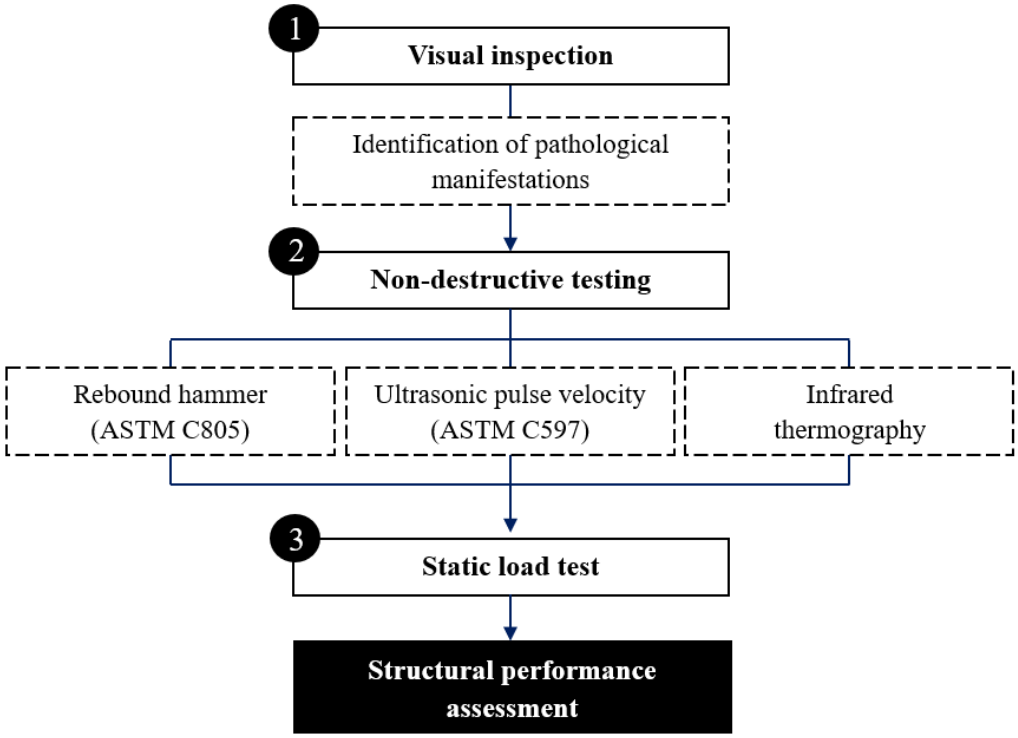

Figure 1. Proposed procedure.

A decision-making framework was established based on the combined interpretation of the results obtained from visual inspection, NDT, and load testing. Three possible scenarios were defined

based on the literature (Harris, 2001; Watt, 2025): (1) suitable for use, when structural elements meet serviceability criteria and do not exhibit significant deterioration; (2) suitable with restrictions, when partial deficiencies are identified but the structure maintains stable behavior under load; and (3) not suitable, when advanced deterioration, low material quality, or non-compliance with reference criteria in the load test is observed. The evaluation considered: (a) the severity of deterioration identified through visual inspection; (b) the material quality estimated from NDT; and (c) compliance with the load test reference criteria according to ACI 318 (American Concrete Institute, 2025).

The complementary approach adopted does not imply the application of all techniques to the same structural elements, but rather the integration of results obtained from different components of the system, considering the practical limitations of each method. In this sense, NDT was applied to beams and columns, while load testing was conducted on slabs, allowing the evaluation of structural response under service conditions. The combined interpretation of results enables a system-level structural diagnosis. Therefore, the complementarity of the approach is based on the assessment of different levels of the structural system—material, element, and global behavior—rather than on a direct point-to-point correlation between techniques applied to the same element.

2.2 Description of the evaluated building

A two-story reinforced concrete building, approximately 20 years old, was evaluated. The structure lacks structural drawings and design calculations. It consists of a system of lightweight slabs supported by reinforced concrete beams and columns. The building is in a rough construction state without roofing, remaining exposed to the environment without protective measures. As a result of prolonged exposure to adverse environmental conditions, the building exhibits an unfavorable state of preservation, evidenced by various pathological manifestations, as described in Section 3.1.

Figure 2 presents the architectural plans of the ground floor and upper floor of the building, in which the evaluated structural elements are identified. The codes used indicate the type of element—column (C) or beam (B)—and the corresponding level—ground floor (G) or upper floor (U); for example, the code CG-1 corresponds to the first column identified on the ground floor.

2.3 Experimental program

2.3.1 Visual inspection

Visual inspection consisted of direct observation and photographic documentation of the surface condition of the building. This stage enabled the identification of structural elements exhibiting pathological manifestations and areas with advanced deterioration, as well as the development of a damage map to locate and classify the main pathologies present in the structure. Visual inspection was conceived as a preliminary qualitative diagnostic stage, aimed at identifying relevant pathological manifestations, critical zones, and potentially compromised structural elements. This information was used to define the locations for NDT application and the selection of slabs to be evaluated through load testing, prioritizing those elements with the greatest evidence of deterioration.

2.3.2 NDT

For rebound hammer testing, a digital Controls hammer, model 58-C0181/DGT, was used following ASTM C805 guidelines (ASTM International, 2018). Due to geometric and accessibility constraints, as well as the limited size of some evaluated areas, the procedure was adapted by applying a regular grid of 3 × 3 impacts per test point. Outliers were discarded according to the criteria established in the standard. Although this adaptation may affect the statistical representativeness of the results, priority was given to obtaining consistent measurements at multiple points within each element. In this sense, the results should be interpreted as indicative

estimates of the surface quality of the concrete rather than absolute strength values. The results correspond to the rebound number (RN) and an indicative estimate of surface compressive strength (CS) provided by the equipment. The interpretation considered the influence of concrete carbonation, evidenced by the presence of reinforcement corrosion and environmental exposure conditions. In this context, an estimated reduction in the range of 30–40% was adopted, based on values reported in the literature (Malhotra & Carino, 2003; Breysse, 2012; Kumavat *et al.*, 2021), and used as a conservative criterion to approximate the effective mechanical strength of the material. This adjustment does not represent a direct measurement but rather an indicative estimate for result interpretation.

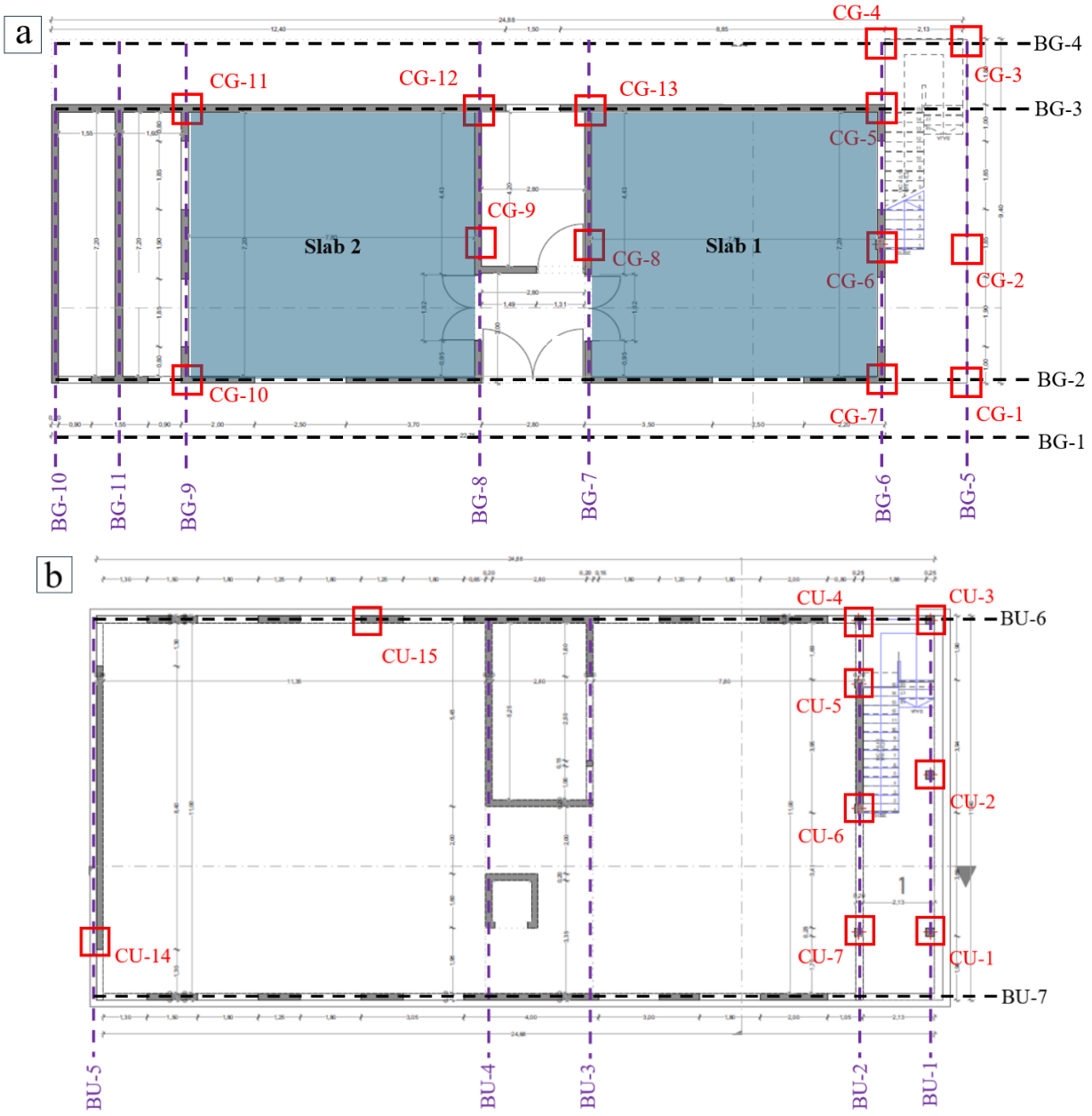

Figure 2. Building plans: (a) ground floor and (b) upper floor.

The UPV test was conducted using a Controls device, model 58-E4900, in accordance with ASTM C597 recommendations (ASTM International, 2016). Measurements were taken at multiple points on the evaluated elements, coinciding with those where rebound hammer testing was performed,

in order to enable direct comparison between both methods. At each point, the ultrasonic wave travel time was recorded and converted into velocity using Equation (1). UPV values were used as indicators of the internal quality of the concrete and the possible presence of heterogeneities, voids, or internal discontinuities (Aquino Rocha *et al*., 2025).

$$UPV = d/t \quad (1)$$

where *d* is the distance between transducers (in m) and *t* is the ultrasonic wave travel time (in s).
As a complement to the previously described NDT methods, infrared thermography was applied using a FLIR thermal camera, model C2, with the objective of identifying thermal anomalies associated with internal deterioration of the concrete, particularly potential cover delaminations (Ichi & Dorafshan, 2022; Ibrahim *et al*., 2026). Infrared thermography was conducted under uncontrolled environmental conditions on an existing structure exposed to the environment in Cochabamba, Bolivia. Measurements were taken during daytime, at an ambient temperature of approximately 22 °C and a relative humidity of 75%, with the presence of solar radiation, which allowed the generation of natural thermal gradients on the surface of the evaluated elements. No artificial thermal excitation procedure was applied; therefore, the analysis is based on passive thermography (Rocha *et al*., 2017).

2.3.3 Static load test

The static load test was conducted on two slabs of the building (Slab 1 and Slab 2), identified in Figure 2. Although the plan dimensions of the slabs are approximately 11.8 × 7.8 m, for testing purposes only the effectively supported dimensions were considered, corresponding to a span of 7.8 × 7.2 m, defined by the actual support conditions of the ground floor. The test was carried out based on the provisions established in Chapter 27 of ACI 318 (American Concrete Institute, 2025) for the evaluation of existing structures, through the gradual and controlled application of a load equivalent to the service load. Under ideal conditions, the test load should be uniformly distributed over the entire slab surface. However, due to practical and logistical constraints inherent to existing structures, as well as the specific characteristics of the evaluated building, an alternative procedure was adopted based on the principle of maximum bending moment equivalence, concentrating the load in a central area of 2.0 × 2.0 m, corresponding to the most critical zone from a structural standpoint.
To determine the equivalent load, a structural analysis was performed using SAP2000, considering a distributed load of 400 kg/m² in addition to the slab self-weight, corresponding to the most critical service load combination according to ACI 318 (American Concrete Institute, 2025). Under this condition, a maximum bending moment of approximately 141 kg·m was obtained (Figure 3a). Subsequently, the magnitude of the concentrated load over the 2 × 2 m area required to reproduce the same bending moment was determined, resulting in an equivalent load of 750 kg/m², thus ensuring equivalence in terms of flexural demand (Figure 3b).

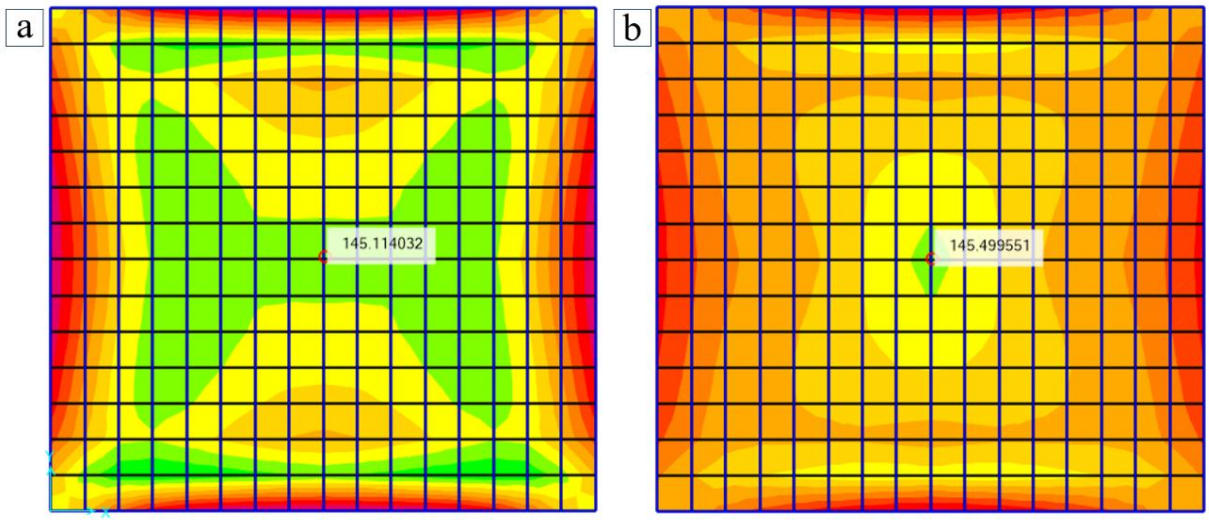

Figure 3. Maximum bending moment: (a) under total load and (b) with the equivalent load of 750 kg/m² applied at the center of the 2 × 2 m area.

The load was applied progressively in eight stages, with increments of 100 kg/m² up to 700 kg/m², followed by a final increment of 50 kg/m² to reach the total test load. Once the maximum load level was reached, it was maintained constantly for a period of 24 hours in order to evaluate the time-dependent behavior of the slab. Subsequently, the system was gradually unloaded, also in eight stages. Figure 4 illustrates the procedure followed during the execution of the load test.

During the test, maximum deflections, the evolution of the element behavior under loading, and elastic recovery after unloading were recorded. For this purpose, a Controls Datalog 8 system, model 58-C0239/A, equipped with four Gefran displacement sensors, identified as S1, S2, S3, and S4, was used. These sensors were strategically placed at the center and at the midpoints of the edges of the 2 × 2 m slab area. The results were evaluated considering reference criteria based on ACI 318 (American Concrete Institute, 2025), including: (a) a maximum absolute deflection of 0.05 in (1.27 mm); (b) the maximum allowable deflection based on the slab span (L/2000 = 7800/2000 = 3.90 mm); and (c) a minimum elastic recovery of 75% after unloading.

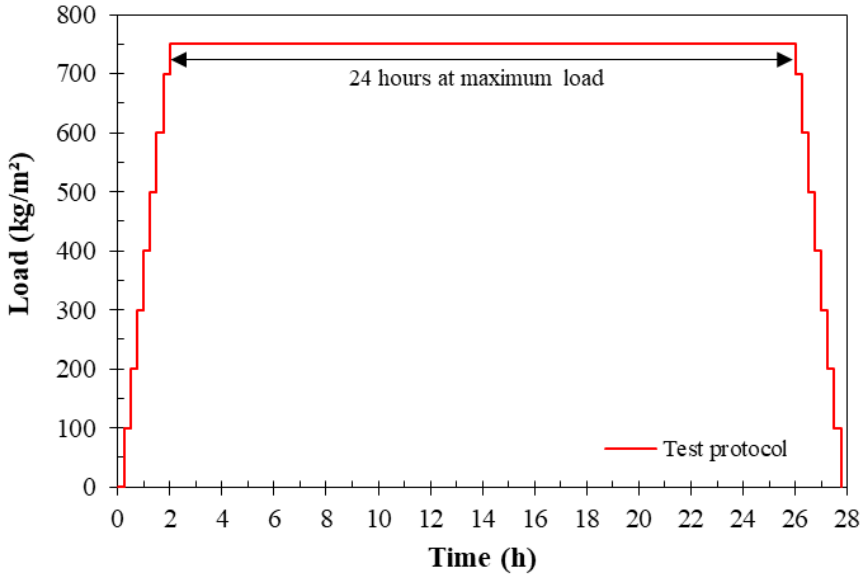

Figure 4. Loading and unloading test protocol.

Although the structural configuration of the slabs can be approximated as predominantly one-way behavior, the evaluation was carried out using general serviceability criteria as a reference for interpreting structural performance, adopting a conservative approach. For the interpretation of the results, a hierarchy of criteria was established, in which compliance with the elastic recovery criterion and the relative deflection limit (L/2000) are considered the primary indicators of structural performance under service conditions, while absolute deflection is used as a complementary criterion. In this sense, an element is considered to exhibit acceptable structural behavior when it satisfies the primary criteria, even if it shows deviations with respect to the absolute deflection criterion.

3. RESULTS

3.1 Visual inspection

Figure 5a shows a general view of the structure, highlighting its direct exposure to the environment. Overall, advanced concrete degradation is observed, characterized by the presence of dark stains associated with moisture and whitish surface deposits, indicating leaching and efflorescence processes (Smith & West, 2021; Nogueira Diniz *et al*., 2023). Additionally, signs of concrete carbonation are evident, along with advanced reinforcement corrosion processes. Figure 5b presents the upper floor slab, where the absence of finishes and protective systems can be observed, as well as a surface directly exposed to environmental conditions. Surface irregularities, accumulation of dirt, and concrete disintegration are identified, conditions that justified the execution of the static load test.

Figure 5. (a) General view and (b) upper floor of the building.

The underside of the slabs shows generalized deterioration (Figure 6), characterized by the presence of dark stains, leaching, and efflorescence. Additionally, areas with surface irregularities and local discontinuities were identified, particularly near supports and beam–column joints, where deterioration is more pronounced. These pathological manifestations indicate prolonged exposure to environmental conditions, mainly moisture, as well as cover detachment, factors that affect material quality and the mechanical response of structural elements (Krentowski, 2021; Richardson, 2023).

Figure 6. Underside of: (a) slab and (b) cantilever.

Figure 7a presents deterioration at beam–column joints, where areas with cover loss, cracking, and alteration of the concrete surface were identified. These regions correspond to critical areas of the structural system, indicating vulnerability of the building in terms of functionality and safety. Figure 7b shows advanced degradation of elements with loss of cover and exposed reinforcement, accompanied by corrosion products. These manifestations confirm carbonation processes in the concrete and prolonged exposure without surface protection (Fuhaid & Niaz, 2022; Poursaee & Angst, 2023). Figure 7c shows stains associated with moisture, surface deposits, and localized material loss, mainly in areas near supports and column connections. In general, these observations confirm an unfavorable condition of the structural elements, justifying the application of NDT and the evaluation of structural performance through static load testing.

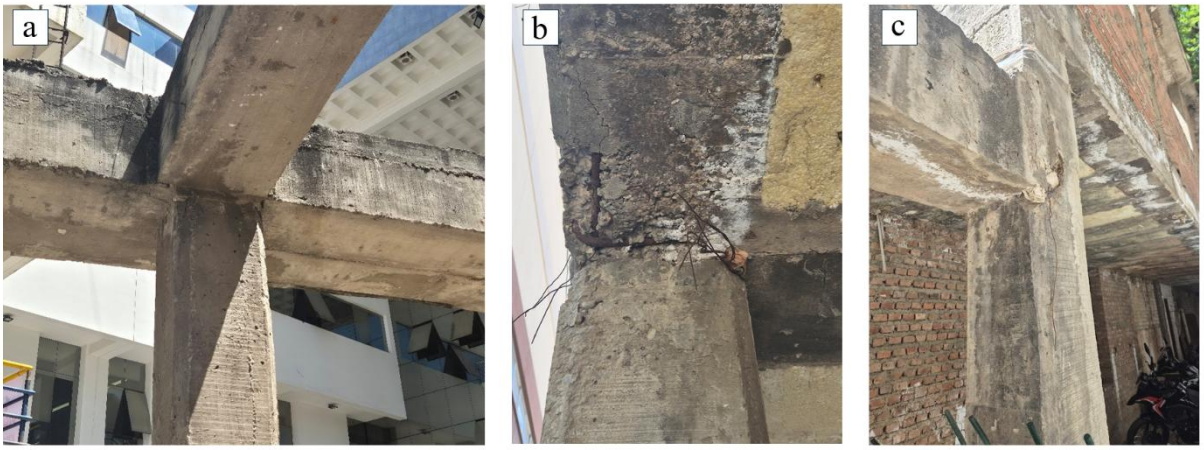

Figure 7. (a) Beam–column joint, (b) reinforcement corrosion, and (c) concrete deterioration.

In order to systematize the information obtained during visual inspection, a damage map of the building was developed, in which the main observed pathological manifestations are identified and located (Figure 8). This map allows the spatial representation of the distribution of pathologies such as moisture, efflorescence, reinforcement corrosion, cracking, and concrete disintegration, facilitating the identification of critical zones within the structural system. In particular, a higher concentration of damage is observed in exposed horizontal elements and in areas near supports and beam–column joints, evidencing a direct relationship between environmental exposure conditions and material deterioration. Likewise, the map guided the selection of points for non-destructive testing and the slabs evaluated through load testing, prioritizing those regions with the highest level

of deterioration. Based on the visual inspection, the main identified pathologies include cover loss, moisture, efflorescence, reinforcement corrosion, and leaching processes, which can be qualitatively classified as moderate to high severity, especially in beam–column joints and elements exposed to the environment. These zones correspond to critical regions of the structural system, where deterioration may compromise steel–concrete bond, load transfer, and the local stiffness of structural elements.

3.2 Rebound hammer and UPV

The selection of the evaluated structural elements was carried out through targeted sampling, based on accessibility criteria and evidence of deterioration identified during the visual inspection (Section 3.1). In particular, elements exhibiting significant pathological manifestations were prioritized in order to assess critical conditions of the structural system. The number of measurement points and evaluated elements was defined considering the actual conditions of the building and the operational constraints inherent to fieldwork, seeking a balance between structural system coverage and execution feasibility. In this sense, the results correspond to a representative evaluation of critical zones rather than an exhaustive statistical sampling of the entire structure.

The results of rebound hammer testing and UPV obtained for columns and beams are presented in Figures 9 and 10, respectively. The CS values estimated from the RN are shown together with the 30% (CS-30%) and 40% (CS-40%) reductions applied to account for the carbonation process, as described in Section 2.3.2.

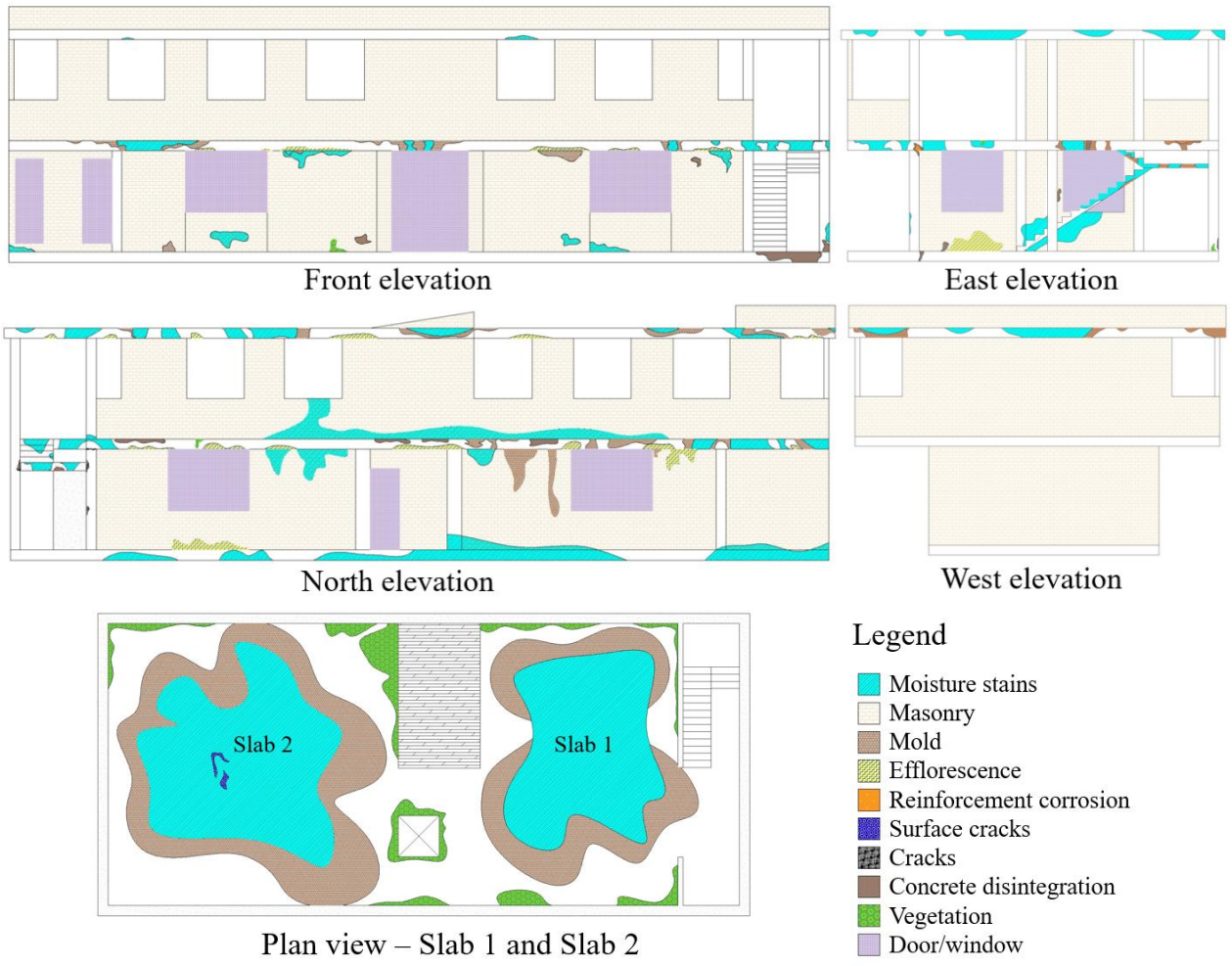

Figure 8. Damage map of the evaluated building.

For columns, both at the ground floor and upper floor levels (Figure 9a and Figure 10a), it is observed that the CS values exceed 25 MPa and, in some cases, surpass 35 MPa, which would generally correspond to concrete strength levels commonly considered suitable for structural applications (American Concrete Institute, 2025). However, the presence of carbonation processes and, consequently, reinforcement corrosion in reinforced concrete indicates that these values do not necessarily reflect the actual condition of the material. The CS was estimated based on rebound hammer testing, which is influenced by concrete carbonation (ASTM International, 2018). This phenomenon is associated with the formation of calcium carbonate ($CaCO_3$) on the surface (Qian *et al*., 2023), which locally increases surface hardness and may lead to an overestimation of CS (Kumavat *et al*., 2021). Additionally, several studies have shown that carbonation can result in apparent or temporary increases in CS in cementitious matrices, associated with microstructural densification and partial pore filling (Lin *et al*., 2025; Rocha *et al*., 2025).

In the case of beams (Figure 9b and Figure 10b), the behavior is similar to that observed in columns, with the difference that the estimated CS values are higher. In most cases, values exceeding 35 MPa were recorded, and in some instances, elements surpassing 45 and 50 MPa were identified. Although these results may suggest high compressive strength, both beams and columns have been subjected to carbonation processes due to continuous environmental exposure for approximately 20 years. This, together with the observed evidence of corrosion, limits the representativeness of these values for assessing actual structural performance.

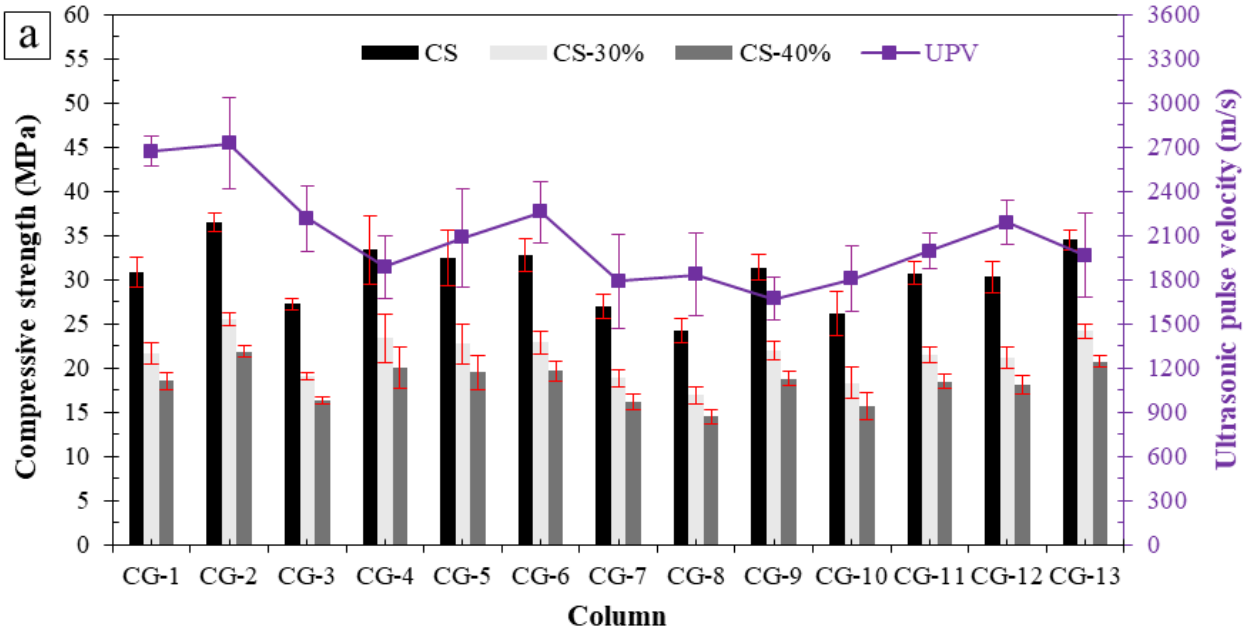

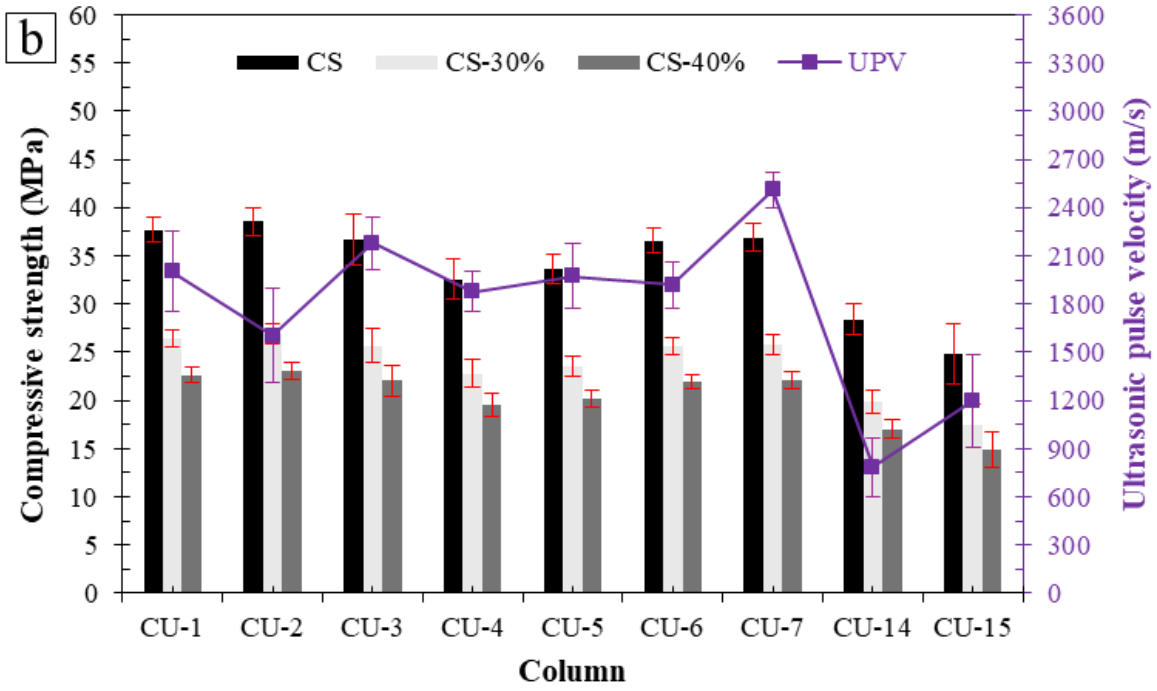

Figure 9. Rebound hammer and UPV results for columns: (a) ground floor and (b) upper floor.

In this context, the CS values estimated for columns and beams were adjusted by applying a reduction in the order of 30–40%, in accordance with recommendations reported in the literature (Malhotra & Carino, 2003; Breysse, 2012; Kumavat *et al*., 2021), in order to approximate the effective mechanical strength of the concrete. Considering this reduction, it is observed that columns reach maximum values on the order of 25 MPa, while a significant number of them exhibit strengths below 20 MPa, suggesting that, in these cases, the concrete may not be suitable for structural purposes (*Ministerio de Transportes, Movilidad y Agenda Urbana*, 2021; European Committee for Standardization, 2021; American Concrete Institute, 2025). In the case of beams, although extreme values approaching 35 MPa are identified, most adjusted values fall within the range of 20 to 25 MPa, suggesting that these elements may still retain a certain load-bearing capacity. Nevertheless, the most critical elements of the system correspond to the columns, as they represent key components in load transfer and overall structural performance, potentially compromising the functionality and safety of the building (*Fédération internationale du béton*, 2020; American Concrete Institute, 2025).

Regarding the UPV test applied to columns, a proportional relationship with the estimated CS values is observed, such that higher CS values correspond to higher UPV values, indicating general consistency between both evaluation methods. However, UPV values are concentrated within an average range between 1750 and 2700 m/s, with additional localized values around 1200 and 900 m/s, which correspond to poor to very poor-quality concrete according to criteria reported in the literature (Cánovas, 1988; Bungey & Grantham, 2006). Although carbonation influenced the rebound hammer results due to its surface nature, the UPV test provided a more representative evaluation of the internal quality of the concrete. In this regard, the results indicate the presence of discontinuities, voids, and possible internal defects, mainly associated with reinforcement corrosion processes and deterioration of the cementitious matrix (Othman & Ayop, 2021; Aquino Rocha *et al*., 2025).

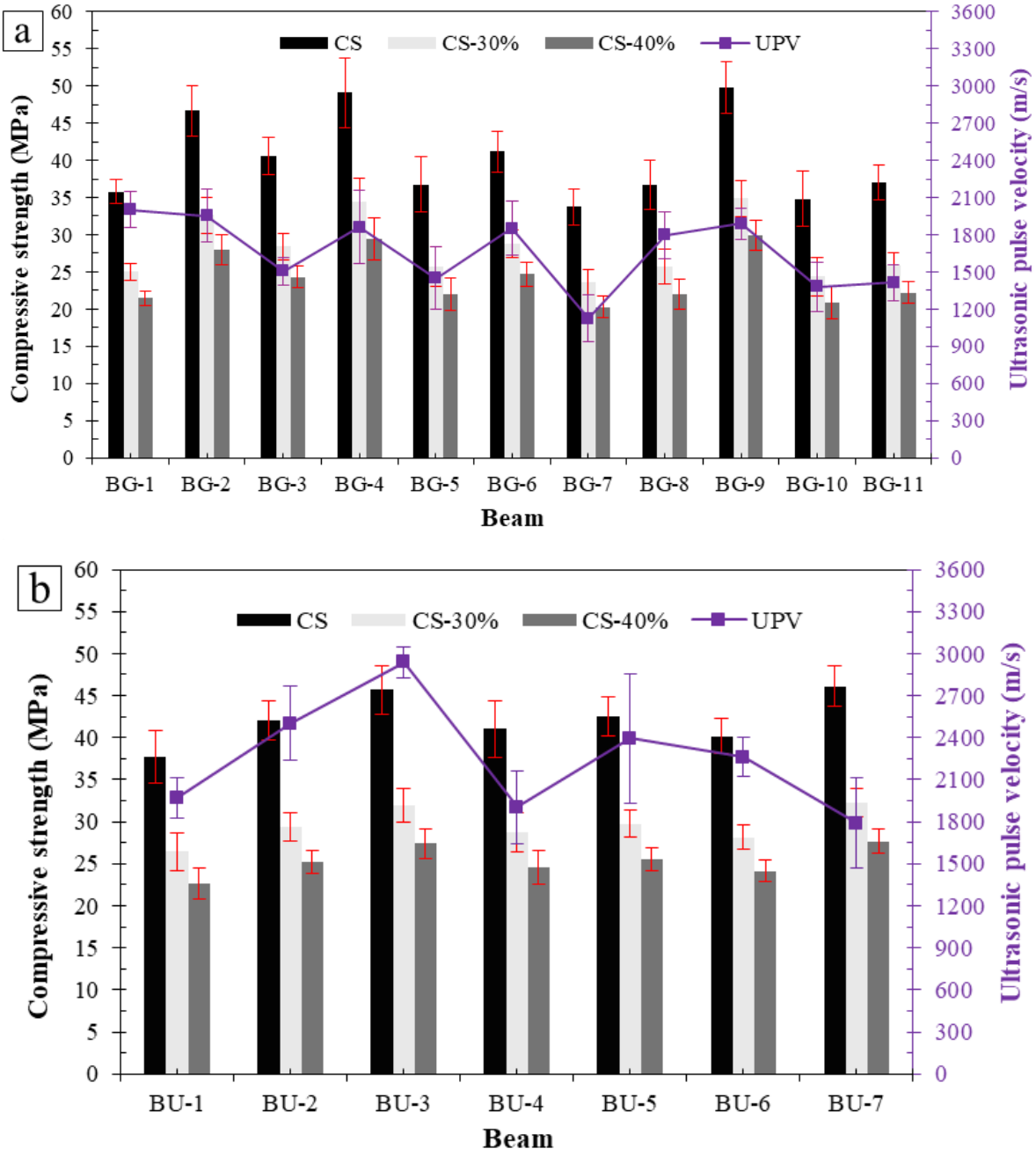

Figure 10. Rebound hammer and UPV results for beams: (a) ground floor and (b) upper floor.

For beams, a behavior similar to that of columns is observed. At the ground floor level, UPV values are generally lower, ranging approximately between 1000 and 2100 m/s, whereas at the upper floor, higher values are recorded, between 1800 and 3000 m/s. However, the dispersion of the data indicates significant material heterogeneity, suggesting that the concrete does not exhibit uniform or adequate quality. Although some regions show relatively higher UPV values, the obtained ranges mostly correspond to categories of fair to very poor-quality concrete (Cánovas, 1988; Bungey & Grantham, 2006). Overall, the combined results of UPV and rebound hammer testing suggest that, while surface strength may be overestimated due to carbonation effects, the internal quality of the concrete is compromised, limiting the actual structural performance of the evaluated elements. The consistency of the results across different points, as well as their agreement with the

visual inspection, reinforces the validity of the adopted interpretation, despite the reduced measurement density.

3.3 Infrared thermography

In addition to rebound hammer and UPV testing, infrared thermography was applied to different elements of the building in order to identify potential internal defects and anomalies. Figure 11a shows a digital image of a beam–column joint, corresponding to the element presented in Figure 7b, where reinforcement corrosion and material degradation are visually evident. In the thermogram (Figure 11b), localized thermal anomalies are identified, characterized by the presence of different thermal gradients. These variations do not follow a uniform thermal pattern but are concentrated in specific regions of the element, coinciding with the deteriorated zones observed in the digital image. In particular, the area identified as SP3 exhibits lower temperatures than the surrounding concrete, suggesting the possible presence of delamination or internal voids, associated with a potential risk of cover detachment (Aquino-Rocha *et al.*, 2024).

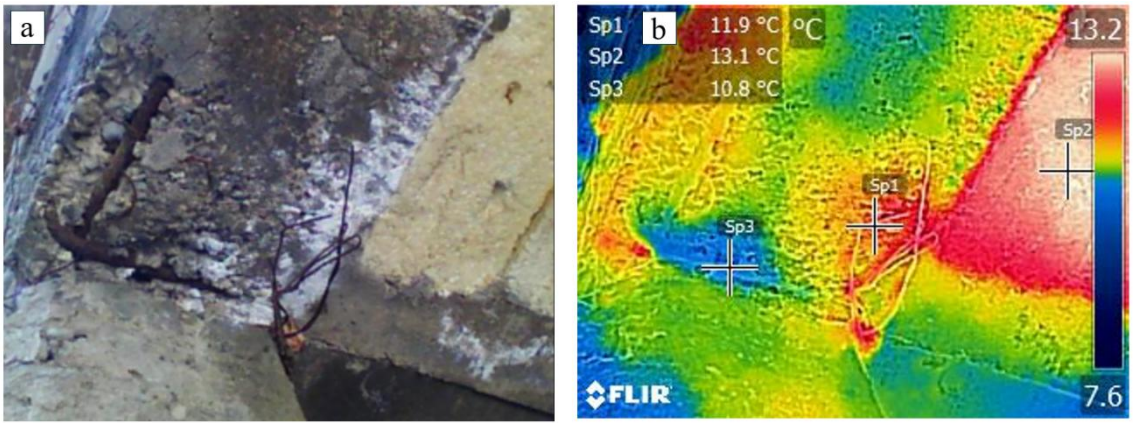

Figure 11. Beam–column joint: (a) digital image and (b) thermogram.

In the case of slab joists (Figure 12a), the corresponding thermogram (Figure 12b) shows differentiated thermal contrasts within the same element (SP1 and SP2), with a temperature difference on the order of 0.9 °C, which allows the identification of possible internal defects (Rocha *et al.*, 2018). These zones coincide with areas where efflorescence, cover loss, and signs of leaching were observed during visual inspection, indicating that the thermal variations are associated with internal degradation processes of the concrete, mainly related to the presence of moisture and loss of material integrity (Avdelidis & Moropoulou, 2004).

Figure 13a presents a digital image of the slab, whose thermogram (Figure 13b) reveals areas with higher surface temperatures compared to their surroundings and a lack of thermal uniformity. This behavior indicates the presence of voids and/or delaminations, as these zones, being directly exposed to solar radiation, tend to heat up more rapidly than intact material due to the interruption of heat transfer, indicating a risk of cover detachment (Aquino-Rocha *et al.*, 2024; Ibrahim *et al.*, 2026). A similar behavior is observed in Figure 14a, corresponding to an element directly exposed to solar radiation. In this case, the thermogram (Figure 14b) shows areas with higher temperatures than the surrounding material, also indicating the presence of internal defects.

The results of infrared thermography should be interpreted qualitatively as indicators of potential thermal anomalies associated with internal defects, rather than as a quantitative assessment of material condition. Despite the absence of controlled conditions, and given that this is a passive technique, the identified thermal anomalies show consistency with the deteriorated zones observed through visual inspection and with the NDT results, thereby reinforcing the validity of the adopted interpretation. Overall, the combined results of infrared thermography, visual inspection, rebound

hammer, and UPV indicate that the identified deterioration is not limited to the concrete surface, but rather corresponds to an internal degradation process, evidencing significant heterogeneity and compromised material integrity.

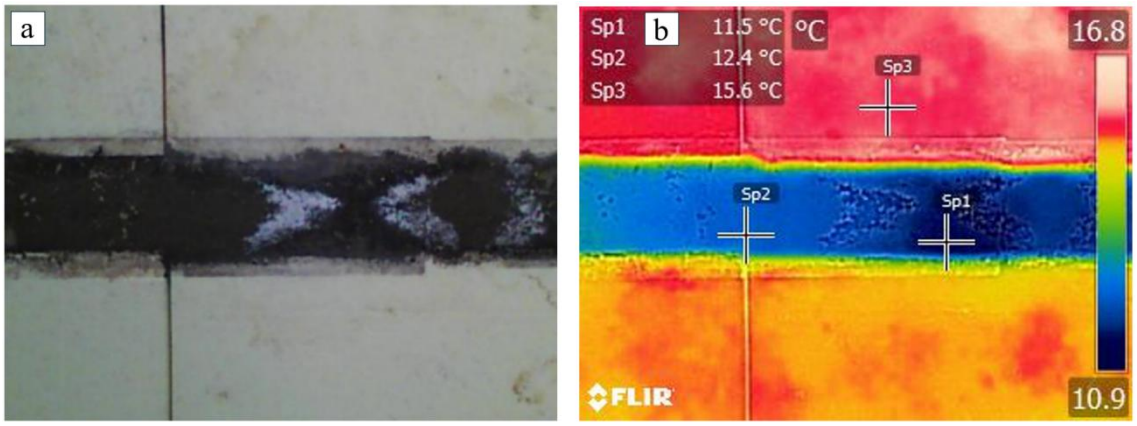

Figure 12. Slab joist: (a) digital image and (b) thermogram.

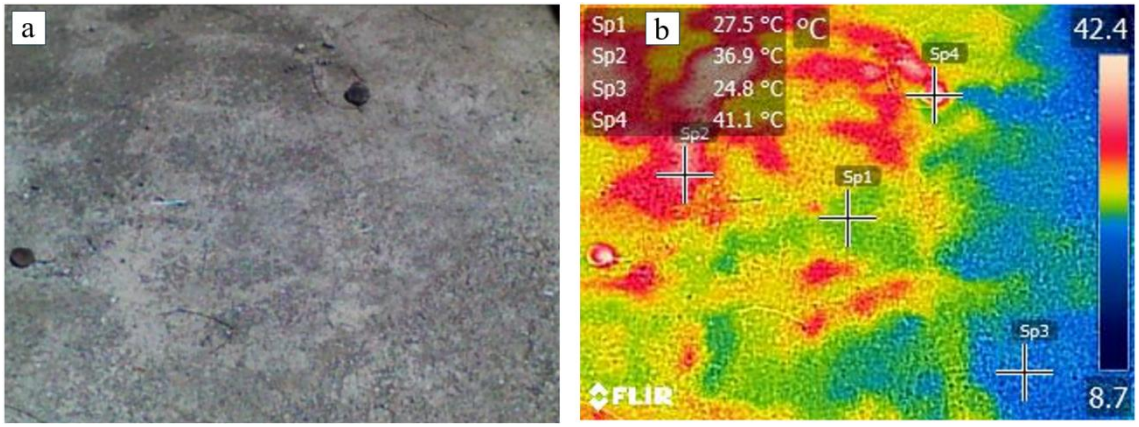

Figure 13. Slab joist: (a) digital image and (b) thermogram.

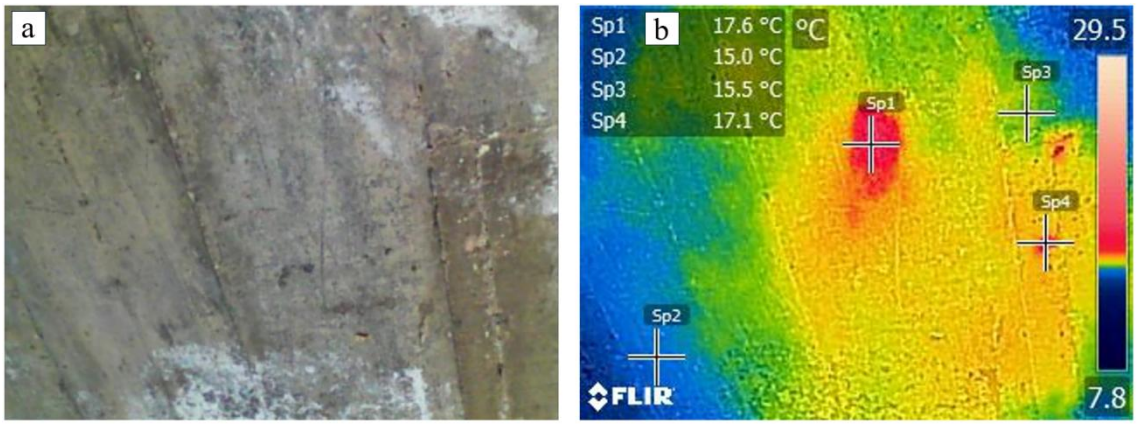

Figure 14. Exposed element: (a) digital image and (b) thermogram.

3.4 Load test

The deflections obtained during the static load test are presented in Table 1 for Slab 1 and Slab 2, where the red color indicates non-compliance with the maximum allowable deflection according to the reference criteria of ACI 318 (American Concrete Institute, 2025), as detailed in Section 2.3.3. Deflections were recorded at each stage of incremental loading, during the 24-hour sustained

loading period, as well as during the gradual unloading process and the immediate elastic recovery of the system. In both slabs, deflections increased continuously and progressively as the load was incrementally applied until reaching the total test load of 750 kg/m² (100%). Figures 15 and 16 show the complete time evolution of the measured deflections for Slab 1 and Slab 2, respectively, including the loading, sustained loading, and unloading phases.

Table 1. Deflections recorded during the static load test.

Load stage	Cumulative applied load (kg/m²)	Slab 1 – Deflection (mm)				Slab 2 – Deflection (mm)			
		S1	S2	S3	S4	S1	S2	S3	S4
Initial	0	0	0	0	0	0	0	0	0
Load 1 (13.33%)	100	0.131	0.238	0.180	0.230	0.369	0.274	0.430	0.420
Load 2 (26.67%)	200	0.336	0.516	0.380	0.510	0.559	0.747	0.830	0.810
Load 3 (40.00%)	300	0.559	0.725	0.580	0.730	0.929	1.147	1.290	1.260
Load 4 (53.33%)	400	0.68	0.874	0.700	0.900	1.314	1.574	1.820	1.780
Load 5 (66.67%)	500	0.88	1.129	0.910	1.170	1.667	2.037	2.330	2.300
Load 6 (80.00%)	600	1.104	1.375	1.080	1.430	2.031	2.531	2.870	2.850
Load 7 (93.33%)	700	1.313	1.633	1.30	1.700	2.395	3.012	3.400	3.390
Load 8 (100.00%)	750	1.378	1.174	1.410	1.820	2.631	3.325	3.750	3.740
After 24 hours	750	1.907	2.205	1.920	2.240	2.928	3.886	4.300	4.260
Unload 1 (93.33%)	700	1.828	2.114	1.830	2.150	2.812	3.687	4.140	4.090
Unload 2 (80.00%)	600	1.634	1.888	1.610	1.920	2.547	3.337	3.780	3.730
Unload 3 (66.67%)	500	1.391	1.633	1.430	1.680	2.272	2.874	3.340	3.330
Unload 4 (53.33%)	400	1.097	1.318	1.230	1.400	2.062	2.413	2.970	2.960
Unload 5 (40.00%)	300	0.817	1.054	0.960	1.110	1.694	2.120	2.540	2.550
Unload 6 (26.67%)	200	0.537	0.731	0.700	0.790	1.361	1.766	2.110	2.120
Unload 7 (13.33%)	100	0.292	0.466	0.420	0.520	1.097	1.350	1.680	1.700
Unload 8 (Final)	0	0.192	0.375	0.340	0.440	0.717	1.046	1.250	1.280
Maximum during test		2.077	2.357	2.016	2.381	3.828	4.565	4.983	4.907

During the 24-hour sustained loading period, an additional increase in deflections was recorded, attributed to the time-dependent behavior of the system. This effect was more pronounced in Slab 2, indicating greater sensitivity to loading and lower overall stiffness of the element. After gradual unloading, partial recovery of deflections was observed, allowing the quantification of instantaneous residual deflection and the degree of elastic behavior of each slab. The recovery percentages and compliance with the criteria based on ACI 318 (American Concrete Institute, 2025) are summarized in Table 2, where green indicates compliance and red indicates non-compliance.

For Slab 1, the maximum recorded deflections ranged between 2.016 mm and 2.381 mm. Although these values exceed the absolute deflection criterion of 0.05 in (≤ 1.27 mm), they comply with the maximum allowable deflection based on the effective span of the slab (≤ 3.90 mm). Likewise, elastic recovery exceeded 75% for all sensors, indicating predominantly elastic behavior, with reduced residual deformations and a stable structural response under the applied test load. In contrast, Slab 2 exhibited unfavorable behavior. Maximum deflections ranged between 3.828 mm and 4.983 mm, exceeding both the absolute deflection limit (≤ 1.27 mm) and the span-based criterion (≤ 3.90 mm) for all sensors. Regarding elastic recovery, only sensors S1 and S2 satisfied the 75% criterion, whereas sensors S3 and S4 showed lower recovery values, indicating more significant residual deformations and partially inelastic behavior. Based on these criteria, Slab 1 demonstrates acceptable structural performance under service conditions, while Slab 2 does not meet the primary criteria, indicating unfavorable structural performance.

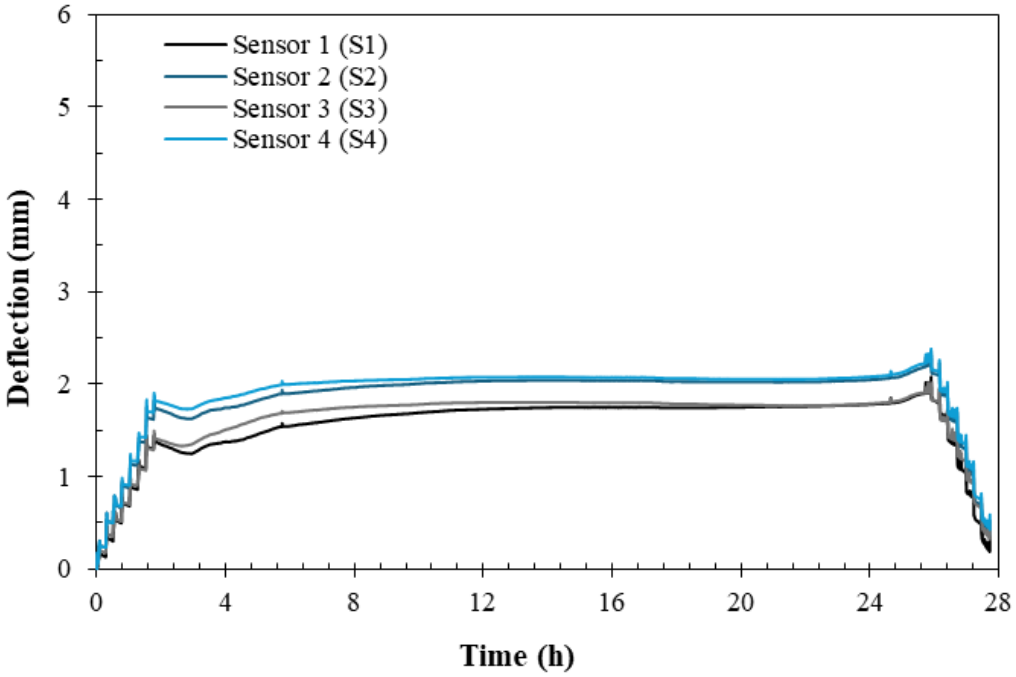

Figure 15. Time evolution of deflection for Slab 1.

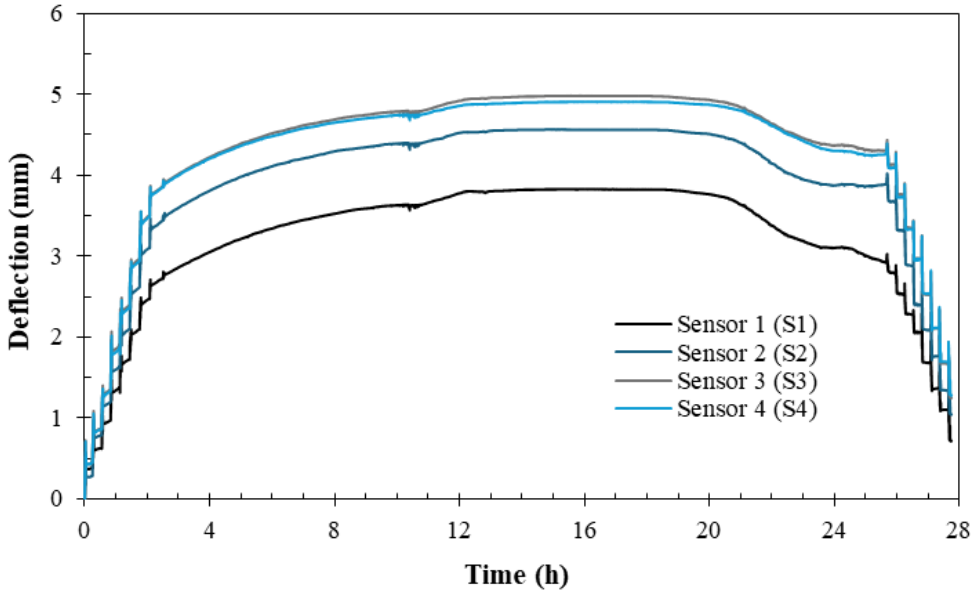

Figure 16. Time evolution of deflection for Slab 2.

Table 2. Acceptance criteria.

Sensor	Slab 1			Slab 2		
	Recovery (%)	Max. deflection		Recovery (%)	Max. deflection	
		≤ 1.27 mm	≤ 3.90 mm		≤ 1.27 mm	≤ 3.90 mm
S1	90.76	Does not comply	Complies	81.27	Does not comply	Does not comply
S2	84.90	Does not comply	Complies	77.53	Does not comply	Does not comply
S3	83.13	Does not comply	Complies	74.91	Does not comply	Does not comply
S4	81.52	Does not comply	Complies	73.91	Does not comply	Does not comply

During the execution of the test, no additional visible cracking was detected in any of the slabs, neither during incremental loading stages, nor during the sustained loading period, nor during unloading. However, the presence of pre-existing cracking and leaching processes limited the visual identification of cracks induced exclusively by the test, without ruling out the possible existence of microcracking or internal damage not observable at the surface. In general terms, Slab 1 exhibited stable and controlled behavior, with a progressive response to load increments and adequate elastic recovery, although it does not satisfy the absolute maximum deflection criterion. In contrast, Slab 2 exhibited excessive deflections, insufficient elastic recovery in part of the evaluated area, and greater sensitivity to sustained loading effects, and therefore does not meet the serviceability acceptance criteria based on ACI 318 (American Concrete Institute, 2025).

The complementarity of results from visual inspection, rebound hammer testing, UPV, infrared thermography, and static load testing enabled a comprehensive assessment of the structural condition of the building. Visual inspection and infrared thermography revealed zones with surface deterioration, thermal anomalies, and internal defects associated with moisture, leaching, and corrosion, consistent with the reduced UPV values recorded, which indicate a loss of internal quality and homogeneity of the concrete. Similarly, static load testing demonstrated that, although some elements exhibit stable behavior under controlled loading conditions, others show excessive deflections and insufficient elastic recovery, reflecting a reduction in service performance.

4. DISCUSSION

The observations obtained through visual inspection and the damage mapping were consistent with the results derived from NDT and load testing, demonstrating that the identified deterioration is not limited to the surface but affects the structural behavior of the building. In general terms, the rebound hammer and UPV results reveal significant variability in material quality, as well as indicative values of reduced strength in several evaluated zones, which is consistent with the deterioration patterns observed during visual inspection. UPV values suggest the presence of internal heterogeneity and potential defects in concrete, which may influence the mechanical behavior of structural elements. Therefore, the consistency between the spatial distribution of deterioration, the reduced material quality identified through NDT, and the structural response observed in the load test allows for a comprehensive interpretation of the structural condition.

Although NDT does not directly provide structural design parameters such as effective compressive strength or modulus of elasticity, the results offer relevant information regarding material quality and its degradation state. In this sense, reduced UPV values, data dispersion, and the potential overestimation of surface strength identified through rebound hammer testing suggest a loss of homogeneity and a reduction in the mechanical properties of the concrete. These conditions are reflected in the observed structural behavior, particularly in Slab 2, where excessive deflections and lower overall stiffness were recorded, consistent with possible mechanical degradation of the material. Therefore, NDT results should be interpreted as qualitative indicators of the structural condition of the material rather than as direct design parameters.

The differentiated application of NDT and load testing responds to the practical conditions of evaluating existing structures. NDT was applied to primary load-bearing elements, such as beams and columns, with the aim of characterizing material quality and detecting potential internal defects, while load testing was conducted on slabs, where it is technically feasible to directly assess structural response under service conditions. In this context, load testing is not intended to directly validate the load-bearing capacity of the elements evaluated through NDT, but rather to provide information on the global structural behavior of the system. Accordingly, the adopted approach is based on the complementarity of evaluation scales (material–element–system), rather than on direct validation between techniques applied to the same structural element.

Due to the absence of detailed structural information and the uncertainty associated with the actual configuration of the load-resisting system, the criteria established in ACI 318 (American Concrete Institute, 2025) were used as a reference for interpreting the observed behavior, rather than as a strict design verification. Therefore, deflection limits and serviceability criteria are used to identify structural performance trends and potential deficiencies under service conditions, adopting a conservative assessment approach. A limitation is acknowledged regarding the uncertainty of the exact structural model of the evaluated slabs, which may influence the precise interpretation of the applied code-based criteria.

The development of a global structural model was not considered in this study due to the high level of uncertainty associated with the evaluated building, which lacks structural drawings, design calculations, and reliable information on material properties and foundation conditions. Under these circumstances, the construction of a numerical model would require multiple assumptions, potentially leading to an unreliable representation of the actual structural behavior. For this reason, the adopted approach prioritizes in situ experimental evaluation through the integration of visual inspection, NDT, and load testing, allowing for direct observation of structural performance under real service conditions. In existing structures with incomplete information, numerical models may introduce more uncertainty than certainty if not properly calibrated.

The combined interpretation of the results allows for a global assessment of the structural condition of the building. Although some elements exhibit acceptable behavior under controlled loading conditions, the presence of advanced deterioration, material heterogeneity, and non-compliance with serviceability criteria in certain elements indicate that the structure does not present uniform or fully reliable performance. In particular, while Slab 1 exhibited stable structural behavior under service loading conditions, Slab 2 did not meet the acceptance criteria, showing excessive deflections and insufficient elastic recovery. Although there is no direct spatial correspondence between all applied techniques, the integration of results is performed at the global structural system level, enabling a coherent interpretation of the overall condition of the structure.

Based on the decision-making framework proposed in the methodology, the structural assessment allows the classification of the building's performance at different levels of suitability. In this regard, Slab 1 can be considered suitable with restrictions, as it exhibits stable behavior under service load conditions, albeit within a context of material heterogeneity and surface deterioration. In contrast, Slab 2 is classified as not suitable due to non-compliance with serviceability criteria, evidenced by excessive deflections and insufficient elastic recovery. At a global level, the building exhibits non-uniform behavior and a compromised structural condition associated with advanced deterioration, material heterogeneity, and the presence of internal defects identified through NDT. From an engineering perspective, the implementation of intervention measures is required, such as more detailed structural assessment, localized strengthening, or rehabilitation, before considering the building suitable for use.

Finally, this study presents some limitations inherent to the evaluation of existing structures with incomplete information. First, no destructive testing through core extraction was performed, which limits the accurate estimation of actual concrete strength and the calibration of NDT results. Likewise, the absence of structural drawings and design calculations introduces uncertainty regarding the configuration of the load-resisting system, support conditions, and actual load paths, restricting the possibility of developing a reliable structural model. Furthermore, NDT results should be interpreted as indicative estimates of material quality, being influenced by factors such as carbonation, moisture, and concrete heterogeneity. The selection of evaluated elements was based on accessibility and visible deterioration and may therefore not fully represent the overall structural behavior. Nevertheless, the integration of results obtained from different techniques allows for a coherent assessment of the global structural condition of the building.

5. CONCLUSIONS

This study evaluated the structural suitability of an existing reinforced concrete building through the complementary application of visual inspection, non-destructive testing (rebound hammer, ultrasonic pulse velocity, and infrared thermography), and static load testing. Based on the results, the following conclusions are drawn:

- Visual inspection revealed an unfavorable state of preservation of the structure, characterized by cover loss, moisture presence, reinforcement corrosion, efflorescence, and leaching processes, which enabled the identification of critical zones within the structural system.
- Rebound hammer and UPV results indicated significant material heterogeneity and reduced strength values. Rebound hammer testing may overestimate surface strength due to carbonation effects, whereas UPV allowed the identification of potential internal defects, in agreement with field observations.
- Infrared thermography enabled the identification of thermal anomalies associated with internal moisture, voids, and possible delaminations, confirming that deterioration is not limited to the concrete surface.
- Static load testing revealed differentiated structural behavior among the evaluated elements: Slab 1 exhibited stable performance under service conditions, whereas Slab 2 did not meet the reference criteria, showing excessive deflections and insufficient elastic recovery.
- The integration of results from visual inspection, NDT, and load testing allowed for a coherent global structural diagnosis, demonstrating that the identified deterioration affects both material quality and structural performance of the building.

Within the adopted decision-making framework, the evaluated structure exhibits non-uniform behavior and an unfavorable structural condition, characterized by advanced deterioration, material heterogeneity, and deficiencies in the service performance of certain elements. In this context, the building should be regarded as globally unsuitable for use without prior intervention, and therefore cannot be considered fully suitable for use in its current condition. Accordingly, a more detailed structural assessment is recommended, along with the implementation of intervention measures such as structural strengthening or rehabilitation of the compromised elements prior to commissioning. Finally, the adopted methodological approach demonstrates that the integration of assessment techniques not only enables characterization of material condition but also supports technical decision-making in high-uncertainty scenarios, such as existing buildings lacking design information.

6. REFERENCES

Abdollahi-Mamoudan, F., Ibarra-Castanedo, C. and Maldague, X. P. (2025), *Non-destructive testing and evaluation of hybrid and advanced structures: A comprehensive review of methods, applications, and emerging trends*. Sensors. 25(12):3635. https://doi.org/10.3390/s25123635

Abedin, M., Basalo, F. J. D. C., Kiani, N., Mehrabi, A. B. and Nanni, A. (2022*), Bridge load testing and damage evaluation using model updating method*. Engineering Structures. 252:113648. https://doi.org/10.1016/j.engstruct.2021.113648

Ali-Benyahia, K., Kenai, S., Ghrici, M., Sbartaï, Z. M. and Elachachi, S. M. (2023), *Analysis of the accuracy of in-situ concrete characteristic compressive strength assessment in real structures using destructive and non-destructive testing methods*. Construction and Building Materials. 366:130161. https://doi.org/10.1016/j.conbuildmat.2022.130161

Alqurashi, I., Alver, N., Bagci, U. and Catbas, F. N. (2025), *A review of ultrasonic testing and evaluation methods with applications in civil NDT/E*. Journal of Nondestructive Evaluation. 44(2):53. https://doi.org/10.1007/s10921-025-01190-0

American Concrete Institute. (2025), *ACI CODE-318-25: Building Code for Structural Concrete — Code Requirements and Commentary*. American Concrete Institute.

Aquino Rocha, J. H., Murillo Borda, W., Herrera Rosas, M. and Cayo Chileno, N. G. (2025), *Comparative Evaluation of Grids for the Detection of Internal Defects in Concrete Using Ultrasonic Pulse Velocity: Experimental Approach*. Journal of Structural Design and Construction Practice. 30(4):04025074. https://doi.org/10.1061/JSDCCC.SCENG-1791

Aquino-Rocha, J. H., Póvoas, Y. V. and Bezerra-Batista, P. I. (2024), *Flaw recognition in reinforced concrete bridges using infrared thermography: A case study*. Revista Facultad de Ingeniería Universidad de Antioquia. (110):99-109. https://doi.org/10.17533/udea.redin.20230521

ASTM International. (2016), *ASTM C597/C597M-16: Standard test method for pulse velocity through concrete*. ASTM International. https://doi.org/10.1520/C0597_C0597M-16

ASTM International. (2018), *ASTM C805/C805M-18: Standard test method for rebound number of hardened concrete*. ASTM International. https://doi.org/10.1520/C0805_C0805M-18

Avdelidis, N. P. and Moropoulou, A. (2004), *Applications of infrared thermography for the investigation of historic structures*. Journal of Cultural Heritage. 5(1):119-127. https://doi.org/10.1016/j.culher.2003.07.002

Boccacci, G., Frasca, F., Bertolin, C. and Siani, A. M. (2024), *Diagnosis of historic reinforced concrete buildings: a literature review of non-destructive testing (NDT) techniques*. Procedia Structural Integrity. 55:160-167. https://doi.org/10.1016/j.prostr.2024.02.021

Bortolini, R. and Forcada, N. (2018), *Building inspection system for evaluating the technical performance of existing buildings*. Journal of Performance of Constructed Facilities. 32(5):04018073. https://doi.org/10.1061/(ASCE)CF.1943-5509.0001220

Breysse, D. (2012), *Nondestructive evaluation of concrete strength: An historical review and a new perspective by combining NDT methods*. Construction and Building Materials. 33:139-163. https://doi.org/10.1016/j.conbuildmat.2011.12.103

Bungey, J. H. and Grantham, M. G. (2006), *Testing of concrete in structures*. CRC Press.

Cánovas, M. F. (1988), *Patología y terapéutica del hormigón armado*. Ed. Dossat.

De Domenico, D., Messina, D. and Recupero, A. (2022), *Quality control and safety assessment of prestressed concrete bridge decks through combined field tests and numerical simulation*. Structures. 39:1135-1157. https://doi.org/10.1016/j.istruc.2022.03.086

Diaferio, M. and Varona, F. B. (2024), *Concrete structures: latest advances and prospects for a sustainable future*. Applied Sciences. 14(9):3803. https://doi.org/10.3390/app14093803

European Committee for Standardization. (2021), *EN 206:2013+A2: Concrete — Specification, performance, production and conformity*. CEN.

Fédération internationale du béton. (2020), *fib Bulletin 90: Visual inspection of concrete structures*. fib.

Fuhaid, A. F. A. and Niaz, A. (2022), *Carbonation and corrosion problems in reinforced concrete structures*. Buildings. 12(5):586. https://doi.org/10.3390/buildings12050586

Ghosn, M., Frangopol, D. M., McAllister, T. P., Shah, M., Diniz, S. M. C., Ellingwood, B. R. and Zhao, X. L. (2016), *Reliability-based performance indicators for structural members*. Journal of Structural Engineering. 142(9):F4016002. https://doi.org/10.1061/(ASCE)ST.1943-541X.0001546

Gupta, M., Khan, M. A., Butola, R. and Singari, R. M. (2022), *Advances in applications of non-destructive testing (NDT): A review*. Advances in Materials and Processing Technologies. 8(2):2286-2307. https://doi.org/10.1080/2374068X.2021.1909332

Harris, S. Y. (2001), *Building pathology: deterioration, diagnostics, and intervention*. John Wiley & Sons.

Ibrahim, A., Faris, N., Zayed, T., Qureshi, A. H., Abdelkhalek, S. and Abdelkader, E. M. (2026), *Application of infrared thermography in concrete bridge deck inspection: current practices, challenges and future needs*. Nondestructive Testing and Evaluation. 41(1):1-44. https://doi.org/10.1080/10589759.2024.2443810

Ichi, E. and Dorafshan, S. (2022), *Effectiveness of infrared thermography for delamination detection in reinforced concrete bridge decks*. Automation in Construction. 142:104523. https://doi.org/10.1016/j.autcon.2022.104523

Krentowski, J. R. (2021), *Assessment of destructive impact of different factors on concrete structures durability*. Materials. 15(1):225. https://doi.org/10.3390/ma15010225

Krentowski, J. R., Knyziak, P., Pawłowicz, J. A. and Gavardashvili, G. (2023), *Historical masonry buildings' condition assessment by non-destructive and destructive testing*. Engineering Failure Analysis. 146:107122. https://doi.org/10.1016/j.engfailanal.2023.107122

Kumavat, H. R., Chandak, N. R. and Patil, I. T. (2021), *Factors influencing the performance of rebound hammer used for non-destructive testing of concrete members: A review*. Case Studies in Construction Materials. 14:e00491. https://doi.org/10.1016/j.cscm.2021.e00491

Lin, L., Xie, M., Li, X., Zheng, K., Wang, J., Yu, K. and Bai, Y. (2025), *Carbonation of cement-based materials under different conditions: From multi-characterizations to mechanism exploration*. Construction and Building Materials. 491:142764. https://doi.org/10.1016/j.conbuildmat.2025.142764

Malhotra, V. M. and Carino, N. J. (2003), *Handbook on nondestructive testing of concrete*. CRC Press.

Ministerio de Transportes, Movilidad y Agenda Urbana. (2021), *Código Estructural*. Gobierno de España.

Nogueira Diniz, J. D. C., Paiva, A. C. D., Junior, G. B., de Almeida, J. D. S., Silva, A. C., Cunha, A. M. T. D. S. and Cunha, S. C. A. P. D. S. (2023), *A method for detecting pathologies in concrete structures using deep neural networks*. Applied Sciences. 13(9):5763. https://doi.org/10.3390/app13095763

Olaszek, P., Łagoda, M. and Casas, J. R. (2014), *Diagnostic load testing and assessment of existing bridges: examples of application*. Structure and Infrastructure Engineering. 10(6):834-842. https://doi.org/10.1080/15732479.2013.772212

Othman, F. Z. and Ayop, S. S. (2021), *Evaluation of corrosion in reinforced concrete: A review on the application of UPV method*. Recent Trends in Civil Engineering and Built Environment. 2(1):160-170.

Poursaee, A. and Angst, U. M. (2023), *Principles of corrosion of steel in concrete structures*. In: *Corrosion of steel in concrete structures*. Woodhead Publishing. 17-34. https://doi.org/10.1016/B978-0-12-821840-2.00004-3

Qian, R., Li, Q., Fu, C., Zhang, Y., Wang, Y., Jin, N. and Jin, X. (2023), *Investigations on atmospheric carbonation corrosion of concrete structure beam exposed to real marine-environment for 7 years*. Journal of Building Engineering. 71:106517. https://doi.org/10.1016/j.jobe.2023.106517

Richardson, M. G. (2023), *Fundamentals of durable reinforced concrete*. CRC Press.

Rocha, J. H. A., Chileno, N. G. C. and Toledo Filho, R. D. (2025), *Mechanical and durability performance of mortars with Portland cement, recycled concrete powder, and metakaolin under accelerated carbonation conditions*. Powder Technology. 453:120616. https://doi.org/10.1016/j.powtec.2025.120616

Rocha, J. H. A., Santos, C. F. D., Oliveira, J. B. D., Albuquerque, L. K. D. S. and Póvoas, Y. V. (2018), *Detecção de infiltração em áreas internas de edificações com termografia infravermelha: estudo de caso*. Ambiente Construído. 18(4):329-340. https://doi.org/10.1590/s1678-86212018000400308

Rocha, J. H. A., Silva, M., Póvoas, Y. and Monteiro, E. (2017), *Análise da profundidade de fissuras em concreto com termografia infravermelha*. Revista de Engenharia e Pesquisa Aplicada. 2(3). https://doi.org/10.25286/repa.v2i3.688

Smith, M. and West, B. N. (2021), *Building pathology*. In: *Building Surveyor's Pocket Book*. Routledge. 89-133.

Watt, D. S. (2025), *Building pathology: Principles and practice*. John Wiley & Sons.